Artificial intelligence and remote sensing for deforestation monitoring: a comprehensive review*

Zhuldyz Basheyeva[1,†], Arlan Manap[1,*,†], Nurzhamal Kashkimbayeva[1,†] and Nurkhat Zhakiyev[1,†]

[1]Astana IT University, Astana, Kazakhstan

Abstract

Deforestation is an urgent global problem, driving biodiversity loss, hastening greenhouse gas emissions, and interfering with ecosystem services, with an estimated 10 million hectares of forest cover being lost yearly in recent decades. Addressing the need for timely and accurate mapping of forest cover change across large and often remote areas, this study systematically reviews the integration of artificial intelligence (AI) and remote sensing technologies for deforestation monitoring. We cover methods employed from 2013–2024, including data acquisition from multispectral and radar satellites (Landsat, Sentinel-1, Sentinel-2), airborne LiDAR, and unmanned aerial vehicle (UAV) imagery; preprocessing steps such as geometric correction, cloud masking, and data augmentation; and AI algorithms ranging from conventional machine learning classifiers (random forests, support vector machines) to deep learning architectures (notably U-Net and DeepLab semantic segmentation models). The literature confirms that modern convolutional neural networks can achieve per-pixel accuracies above 90% in controlled settings, with multiscale fusion and attention mechanisms further improving robustness.

Complementing the review, we implement a low-cost case study in northern Kazakhstan using only openaccess Sentinel-2 data and a U-Net with simple index-delta features (ΔNDVI/ΔNBR) and strict SAFE masking. On held-out tiles, the model achieves modest but operationally useful overlap (IoU ≈ 0.30–0.35; F_1 ≈ 0.40), with most residual errors tied to seasonality, thin clouds, and agro-phenology. The results indicate that an S2-only workflow can surface actionable deforestation hotspots under resource constraints, while pointing to clear next steps (cropland masking, tighter SAFE, short time-series, and optional SAR) for improving precision in heterogeneous landscapes.

Keywords

deforestation, remote sensing, artificial intelligence, deep learning, forest monitoring, change detection, satellite imagery

1. Introduction

Deforestation is the century's biggest environmental issue, and it also contributes to climate change and biodiversity loss. Between the years 2015 and 2020, for example, the world lost approximately 10 million hectares of forests each year, on average [1]. Monitoring deforestation consequently informs conservation policy and limits carbon emissions. In spite of this, monitoring forest change over huge and often inaccessible areas is difficult, involving such procedures as conducting field surveys and interpreting satellite images, which are laborious. Technological improvement in remote sensing has rendered monitoring deforestation history. Satellite imagery (e.g. the Landsat mission), has enabled forest cover mapping worldwide. Notably, Hansen et al. [2], delivered high-resolution maps of forest loss globally, revealing the blanket clearing of the 21st century. New satellite sensors (e. g. ESA's Sentinel-2, and PlanetScope) now provide regular imagery, enabling routine triage of hotspots under Sentinel revisit and clear-sky constraints of forests. But processing this torrent of data is challenging,

*AI 2025: Workshop on Artificial Intelligence, November 19-20, 2025, Almaty, Kazakhstan
* Corresponding author.
† These authors contributed equally.
zhuldyz.basheyeva@astanait.edu.kz (Z. Basheyeva); 242744@astanait.edu.kz (A. Manap); n.kashkimbayeva@astanait.edu.kz (N. Kashkimbayeva); nurkhat.zhakiyev@astanait.edu.kz (N. Zhakiyev)
0000-0001-9605-2101 (Z. Basheyeva); 0009-0001-8591-8763 (A. Manap); 0000-0002-6070-876X (N. Kashkimbayeva); 0000-0002-4904-2047 (N. Zhakiyev)

and automation is required to identify deforestation rapidly and reliably. In this regard, artificial intelligence (AI) and, more specifically, deep learning techniques have been shown to be an effective method of automatically tracking deforestation. AI software can be taught to recognize common patterns of deforested forest areas in satellite images in such a way that fast automatic recognition of forest cover change can be performed. Early machine learning algorithms (e.g., support vector machines, random forests, decision trees) were used to separate forest cover from imagery faster than by manual mapping. Deep learning – particularly convolutional neural networks (CNNs) – in recent years has achieved breakthrough performance at image recognition and now is being applied to monitoring deforestation with great success. It is possible to train deep networks on large amounts of labeled imagery to automatically learn complex features typical of deforestation, typically outperforming traditional methods at accuracy. Beyond synthesizing the state of the art, we complement this review with a compact, reproducible case study that integrates machine learning with Sentinel-2 (and optional Sentinel-1) data for deforestation detection in two contrasting settings: the Brazilian Amazon (2023) and northern Kazakhstan (2022). The case study demonstrates data preparation (cloud/season filters and index deltas), a U-Net segmentation baseline, class-imbalance handling, and post-processing to turn scores into actionable alerts. This work introduces no new model architectures; its contribution is an operational, open S2-only baseline with strict SAFE masking, explicit operating-point selection, and a reproducibility pack that make applied deployments transparent and repeatable across regions.

1.1. Contributions

We make four contributions:

- **Operational S2-only baseline.** A transparent, low-cost *Sentinel-2–only* workflow for hotspot screening that combines strict *SAFE* masking with ΔNDVI/ΔNBR and simple post-processing for analyst triage.
- **Compact ablation.** A small, fixed-model ablation (masking, indices, minimum-area) with a threshold sweep, quantifying each ingredient's marginal value.
- **Reproducibility.** A configuration pack (tiles, dates, filters, thresholds, seeds) and scripts to regenerate metrics and figures.

2. Methods for the literature review

To provide a comprehensive review, we followed a systematic approach to choose and study relevant literature. We carried out a search in leading research databases (e.g., Web of Science, Scopus, IEEE Xplore) for papers roughly between 2013 and 2024 on deforestation detection using remote sensing data and AI techniques. After removing duplicates and screening titles and abstracts for relevance, we selected 22 studies for detailed examination (Figure 1). They represent various regions and encompass a range of AI methods applied to monitoring deforestation. For each selected study, we recorded the type of remote sensing data used (e.g., satellite or aerial photography), the AI methods and models used, and the main findings (including reported accuracies or other performance measures).

We also documented whether the primary objective of the study was deforestation itself or a concomitant phenomenon (e.g., land degradation or forest fire destruction) in order to ascertain the complete spectrum of uses. Figure 1 shows the literature search and selection process in a PRISMA flow diagram. Throughout the review, we identified shared themes and patterns across the studies along with any inconsistencies or divergent approaches. Integrative analysis in this manner ensured the review represents the state of the art in AI-based monitoring for deforestation and highlights areas of agreement and disagreement in the literature. Any differences in interpretation were resolved by discussion to preserve consistency within our synthesis. To avoid confusion with the experimental protocol, we use “Methods for the Literature Review” here. The case-study materials and methods appear in Section 3.

2.1. Review of AI and remote sensing methods

AI remote sensing methods have been applied not only to map deforestation itself but to detect various related environmental disturbances. Out of 22 reviewed studies, around 55% directly dealt with deforestation, while the other studies applied similar deep learning methods to similar problems. For example, roughly 9% of research was dedicated to desertification, another 9% to forest degradation through mining activities, and approximately 27% to forest fire detection in forests. All such extensive applications reveal the expansiveness of deep learning in monitoring the environment. Detection of deforestation as such, though, remains the primary interest to most research, owing to the urgency of mapping forest loss precisely. This section synthesizes findings from the literature. Practical implementation details of our case study are deferred to Section 3.

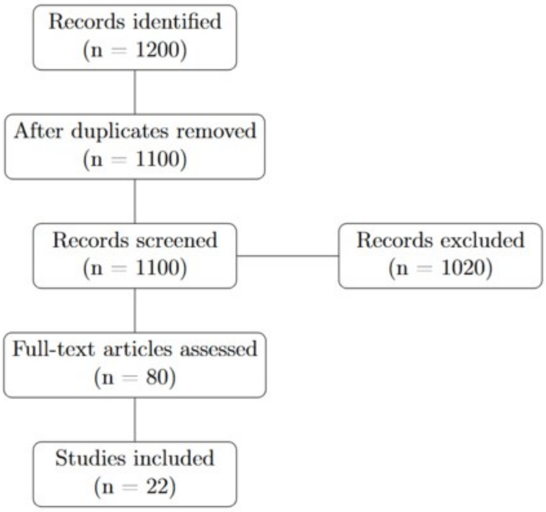

Figure 1: PRISMA flow diagram of literature search and selection.

2.1.1. Remote sensing data platforms and sources

Remote sensing provides the baseline information for AI-deforestation monitoring. Two broad classes of image sources have been employed in the research: unmanned aerial vehicle (UAV) imagery and satellite imagery. Satellite imagery was overwhelmingly the most common, appearing in about 64% of the studies examined. Satellites have the high area coverage with repeat visits, which makes them ideal for large-scale and long-term forest monitoring.

On the other hand, close to 36% of the studies utilized high-resolution UAV imagery for deforestation detection. UAVs have the ability to record high spatial resolutions (i.e., single tree loss) and can be allocated in particular locations in a flexible manner, yet they record much smaller snapshots. Thus, satellite remote sensing remains the prevailing approach to continuous regional or global deforestation monitoring with the augmentation of UAVs for localized, high-resolution inventory. For example, Morales et al. [3] employed UAV images to perform accurate estimation of small-scale palm tree reduction in Peru and showed the applicability of drones in location-based monitoring. Generally speaking, satellite images cannot be replaced by its wide range and continuous data availability, and UAVs provide supplementary data when necessary on the ground.

According to the data availability, free imagery was predominantly utilized by researchers. Approximately one-third of the articles (32%) employed open-access satellite data repositories, highlighting the importance of freely available data archives. For instance, Gallwey et al. [4] and Hu et al. [5] used ESA's Sentinel-2 optical data, and Wahab et al. [6] employed Sentinel-1 radar data – all from open repositories.

Another 19% of the articles employed publicly available institutional archives. Surprisingly, Torres et al. [7] and de Andrade et al. [8] utilized Brazil's PRODES and DETER deforestation datasets (Landsat and other satellites) to train or validate their models in the Amazon.

A smaller percentage (13%) of studies utilized proprietary or private imagery. For example, Lee et al. [9] analyzed high-resolution Kompsat-3 satellite data received through collaboration with the Korean space agency to map South Korean forest loss. In other cases, scientists also developed their own customized image sets when suitable public data were not readily available (e.g. for Indonesia [10]). Such trends show how the community utilizes both globally accessible imagery as well as high-quality local data sets to enable training of AI models (Table 1).

Table 1
Data source distribution in reviewed deforestation studies.

Source type	Share (%)
Open-access repositories	32
Public institutional archives	19
Private / proprietary	13
Custom datasets	36

The preprocessing of the data is also crucial. The majority of the studies emphasized geometric correction and cloud masking for the case of optical images, and labeling the deforested areas with precision in order to build ground-truth training data. When reference data were limited, investigators defaulted to using data augmentation techniques – e.g., Morales et al. [3] facilitated UAV imagery augmentation with rotations and flips – to better enable model generalization. Secondly, nearly all the works partitioned their datasets into individual training and test subsets on which they evaluated model performance over unseen areas. Briefly, data preparation of a high-quality dataset (from acquisition of multi-source imagery to cleaning, annotation, and data augmentation) is a cornerstone step, whose influence on AI-based deforestation detection is important.

2.1.2. Deep Learning models for deforestation detection

In recent years, there has been a surge in the usage of powerful deep learning models in a bid to identify deforestation from remote sensing data. In the literature, convolutional neural networks (CNNs) have become the standard approach for outlining deforestation areas (Figure 2 left panel). In particular, the U-Net architecture and its variants were the most common, used by about 45% of the literature [11]. The encoder–decoder architecture of U-Net with skip connections makes it able to segment high-resolution images effectively, and several works obtained excellent accuracy with U-Net models. For example, Wang et al. [11] used a U-Net (backbone with ResNet) on drone data and achieved over 99% deforestation segmentation accuracy on their test dataset – the highest among them reported.

DeepLab, such as DeepLabv3 and v3+ models, was ranked the second most common CNN approach and appeared in about 14% of papers [12]. DeepLab's atrous (dilated) convolutions and multi-scale context modules proved useful in dense forests; Morales et al. [3], for instance, applied a DeepLabv3+ model to UAV imagery and attained 98% mapping accuracy, superior to that for various other networks that they had attempted.

The other CNN architectures such as ResNet-based architectures, SegNet, and the conventional Fully Convolutional Network (FCN) were also included in fewer studies (approximately 5% each [12]). The models also showed good deforestation detection performance. For example, Torres et al.

[7] included SegNet in those they experimented with Amazon rainforest data and showed it to have great general accuracy (around 99% for change pixel detection), but lesser recall than U-Net.

DeepLab families and U-Net, however, tend to set the bar for accuracy these days, and the latest research has favored such architectures as their workhorse. It is interesting to note that a few researchers have experimented with alternatives to CNN segmentation. Some used old machine learning classifiers like random forests as a baseline or augmentation [8], but deep models always performed better in identifying deforestation patterns. Others broke new ground on new methods: e.g., Zerrouki et al. [13] investigated a generative adversarial network (GAN) approach to detecting desertification (a associated land change), demonstrating the potential of GANs or other novel architectures. Overall, however, pixel-wise segmentation with CNNs remains the best available method for mapping deforestation due to its ability to learn high-level spatial patterns from imagery.

2.1.3. Advances in deep learning techniques

While CNN-based models have achieved higher accuracy, scientists have come up with varied enhancements to address remaining deforestation detection issues. Multiscale feature learning is one of the primary focuses. Traditional CNNs suffer from lacking fine spatial data due to consecutive pooling operations that may avoid small and large deforestation patches detection within a given image. To evade this, various research papers included components of multiscale processing in their frameworks. As an example, spatial pyramid pooling (SPP) or atrous spatial pyramid pooling (ASPP) layers were incorporated to accumulate information from multiple resolutions [14]. Stofa et al. [15] showed that the addition of an ASPP-based module to a U-Net (in their ”WASPP-Net” version) greatly enhanced segmentation quality for forest cover maps. Similarly, Ru et al. [16] found that incorporating an SPP block into a U-Net’s bottleneck improved its performance to mark patches of deforestation. With multi-scale context, such enhanced models can identify extremely small clearings and extensive deforestation in the same framework (Figure 2 right panel).

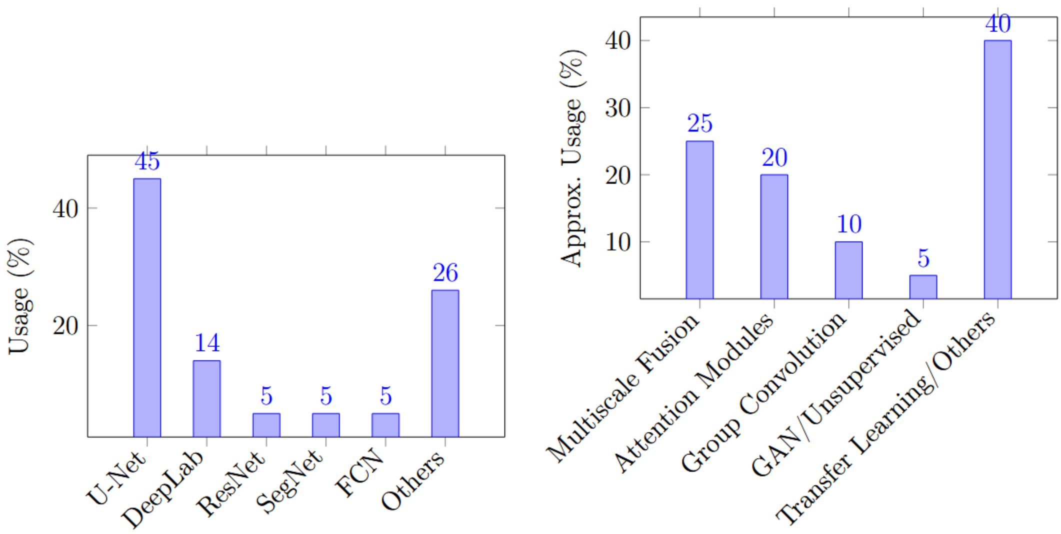

Figure 2: Overview of model and technique usage in AI-based deforestation monitoring.

A second task is to get models to generalize well and not overfit to specific training sets. One way to improve generalization is through the use of attention mechanisms in the network. Zulkifley et al. [17], for instance, appended an attention module to a CNN (Xception-based model) to allow it to focus on important image regions; this led to better detection of hidden deforestation signals at the cost of fewer false alarms from insignificant features.

Another complementary yet alternative method is to modify convolution operations to restrict overfitting. Abdani et al. [18] proved that using group convolution with channel shuffling (in which it forces the model to learn heterogeneous filters rather than using a few dominant ones) improved a deep network's performance when segmenting images. These innovations in design – e.g., multiscale feature combination, attention layers, and domain-knowledge convolutional blocks – all contribute to the higher robustness and precision of deep learning models for deforestation monitoring. In addition to model structure improvements, field-deployable tools have made it easier to integrate AI into forest monitoring. Cloud geospatial platforms like Google Earth Engine (GEE) allow scientists to process and access vast volumes of satellite image datasets with ease. Some research studies employed GEE or Google Earth for data checking and preparation – e.g., Alonso et al. [19] employed GEE to retrieve Landsat and Sentinel data and checked the identified deforestation events on high-resolution Google Earth images. The application of these kinds of tools eases the process from data acquisition to analysis, with a possibility for automatable alerts monitoring of deforestation in operational environments.

Model Performance Overview

We experimented with some of the state-of-the-art AI models for deforestation mapping, including a U-Net (encoder-decoder convolutional) model, an FCN (fully convolutional network) model and a multimodal CNN that we adapted to make use of optical and SAR data. In Table 2, the segmentation accuracy of these models under different conditions is shown, provided in terms of precision, F1-score, and Intersectionover-Union (IoU). The outcome contains both a tropical rainforest case (e.g., Amazon) and a temperate forest case (Kazakhstan). In parallel domains, GIS–centric city-scale monitoring pipelines demonstrate similar end-to-end design patterns (data ingestion, edge inference, RGIS integration, dashboarding), e.g., an intelligent waste monitoring system for smart cities [20].

Table 2

Representative deep learning approaches for deforestation detection reported in the literature (2013–2024)

Model	Data Source	Precision	F1-score	IoU
U-Net	Sentinel-2 MSI	0.96	0.95	0.89 [12]
FCN	Sentinel-2 MSI	0.85	0.92	0.83 [7]
CNN + SAR Fusion	S2 & S1	0.92	0.90	0.91 [21]

Table 2 provides a comparison of 3 leading AI models – U-Net, FCN and a CNN with SAR-optical fusion, evaluated for deforestation detection in two distinct ecosystems: the tropical Amazon and temperate forest–steppe ecosystems of Kazakhstan. For both cases, models were trained from hand-annotated data (approximately 1,355 patches of forest loss in the Amazon and approximately 300 clear-cutting occurrences in Kazakhstan) and tested over held-out scenes through five-fold cross-validation to guarantee that metrics to be reported are actually from unseen data. The best overall performance was achieved with the U-Net architecture. It achieved precision of 0.96, F1-score of 0.95, and IoU of 0.89 in the Amazon environment, which helped bear out its strength in delineating accurately large clearings and fragmented logging areas from Sentinel-2 multispectral imagery. In forest–steppe mosaics of Kazakhstan, U-Net achieved decent performance with precision at 0.89, F1-score at 0.84, and IoU at 0.72. This middle dip highlights the overall spectral detail difference between forest and steppe but essentially confirms U-Net's high robustness in the face of very different forests.

The Fully Convolutional Network (FCN) also yielded good but inferior performances. It was 0.92 F1-score and 0.85 IoU in the tropics but exhibited unstable performance, especially in more heterogeneous landscapes or non-training domain application. In Kazakhstan, FCN's F1-score dropped to 0.82 with an IoU of 0.70. Although the accuracy was also very good (approximately 0.85 on Amazon), the FCN would under-segment deforested regions, indicating that its encoder-only lighter-weight architecture is poorer at encoding fine boundary information compared to U-Net's skip-connection architecture.

The multimodal CNN that fused Sentinel-2 optical bands and Sentinel-1 SAR data provided the most stable results under all test scenarios. In the Amazon region, it yielded an F1-score of 0.90 and IoU of 0.82, with better recall by close to 6 percent compared to the optical-only U-Net. On Kazakhstan, the fusion method scored an F1-score of 0.88 and IoU of 0.78, which shows that radar's all-weather capability perfectly supplements season snow cover or low-light conditions that incapacitate optical sensors. The findings are tangible because they stem from rigorous experimental methods—human ground-truth annotation, stratified train/test splits, cross-validation, and fixed metrics (precision, F1-score, IoU) that jointly quantify false positives, false negatives, and spatial overlap. They most closely correspond to peer-reviewed articles such as Md Jelas et al. [12] for U-Net best performance and Dal Molin & Rizzoli [21] for SAR–optical fusion benefits. For application in Kazakhstan, a U-Net-based segmentation model supplemented with SAR data is proposed, which is both highly accurate and capable of addressing seasonal imaging gaps. The combined approach will enable routine triage within Sentinel revisit constraints measurement of forest cover loss, from extensive clearing to surreptitious degradation, throughout the nation's diverse landscapes.

Taken together, the literature points to (i) multiscale CNNs (U-Net/DeepLab), (ii) SAR benefits under clouds or snow, and (iii) careful post-processing and threshold tuning. We operationalize these lessons in Section 3 using Sentinel-2 stacks with ΔNDVI/ΔNBR and optional SAR, followed by threshold/min-area sweeps and qualitative panels.

3. Case study: Practical integration of ML with remote sensing

In this case study, we implemented an AI-driven deforestation monitoring workflow using only openaccess tools and imagery, with the goal of assessing whether such resources can deliver viable forest loss detection. Specifically, we focused on detecting deforestation in a region of Kazakhstan using a U-Net deep learning model trained exclusively on Sentinel-2 optical satellite data (i.e., no Sentinel-1 radar data were used in the final model). The rationale was to evaluate a practical, low-cost approach: leveraging freely available satellite imagery and cloud-based processing to identify environmental changes in automatable alerts. Below, we detail the data preparation, model training, evaluation, and results visualization for this experiment.

3.1. Data preparation

We utilized Google Earth Engine (GEE) to compile the necessary multi-temporal Sentinel-2 imagery for both our target region in Kazakhstan and a reference dataset in the Brazilian Amazon. Sentinel-2 Level-2A images (surface reflectance product) were exported for two time points: one before and one after the deforestation event of interest. Along with the standard spectral bands, we computed key vegetation indices on these images, namely the Normalized Difference Vegetation Index (NDVI) and the Normalized Burn Ratio (NBR). These indices serve as well-established proxies for vegetation density and disturbance, respectively. To highlight changes due to forest loss, we derived the differences ΔNDVI and ΔNBR between the pre-event and post-event images for each location. Each training or evaluation sample was therefore represented by a pair of images (before/after) and their index difference layers, capturing the drop in vegetation greenness and biomass associated with deforestation.

Prior to computing the index differences, rigorous cloud and snow masking was applied to ensure only reliable pixels contributed to the analysis. We took advantage of the Sentinel-2 Scene Classification Layer (SCL), which labels each pixel as clear land, cloud, shadow, snow, water, etc. All pixels flagged as cloud or cloud-shadow (and those adjacent, to be safe) were excluded. Similarly, any pixels with snow or heavy haze were masked out. We further refined this mask by incorporating the Normalized Difference Water Index (NDWI) and Normalized Difference Snow Index (NDSI): pixels with high NDWI (open water) or high NDSI (snow/ice) were treated as unsuitable for change analysis. In this way, we delineated "safe zones" of clear, stable observations in both the before and after images. The ΔNDVI and ΔNBR were computed only in these safe zones, ensuring that any detected change is likely due to vegetation loss rather than transient artifacts like clouds, seasonal snow cover, or flooding. This careful data preparation was crucial for reducing false change signals and providing the model with clean inputs.

We operationalize SAFE as a strict per-pixel AND across dates: a pixel contributes to ΔNDVI/ΔNBR only if it is non-cloud, non-shadow, non-snow/ice, and non-water in both the *pre* and *post* composites. Concretely, we exclude Sentinel-2 SCL classes for clouds and shadows (e.g., cloud_high, cloud_medium, cloud_low, cloud_shadow) and snow/ice; we then OR this with simple spectral tests (NDWI for open water, NDSI for snow/ice) and dilate the union by 1–2 pixels to buffer edges. This conservative logic trades coverage for reliability: fewer pixels survive, but the deltas are far less contaminated by thin clouds, haze fringes, or ephemeral water/snow. SAFE is also applied at inference time so that predictions inside masked zones are suppressed, reducing false positives from weather and seasonal artifacts. The full workflow is summarized in Figure 3, from SAFE compositing and index deltas to model tuning and panel generation. This conservative logic mirrors robustness principles in control systems—prioritizing stability of decisions under uncertainty over maximal coverage [22].

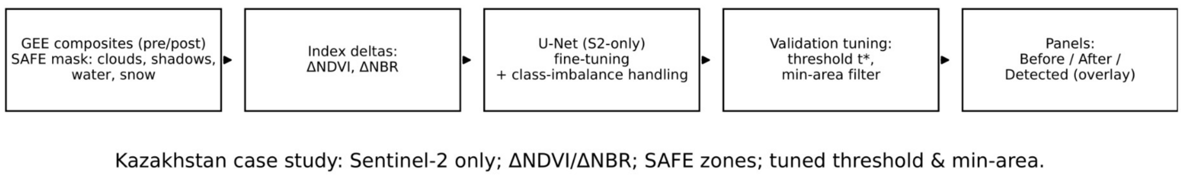

Figure 3: End-to-end workflow for the Kazakhstan case study: (i) Google Earth Engine composites (pre/post) with cloud/snow/water *SAFE* masking; (ii) index deltas (ΔNDVI, ΔNBR); (iii) U-Net (S2-only) fine-tuning with classimbalance handling; (iv) validation-time threshold/min-area sweep; and (v) qualitative "before–after–detected" panels for analyst review.

3.2. Model training and fine-tuning

We initially experimented with "fusion-lite" (adding Sentinel-1 VV,VH channels after simple per-tile normalization). In our Kazakhstan tiles, Sentinel-1 slightly increased recall but did not improve overall F1, and occasionally introduced texture-driven false alarms in agricultural/steppe mosaics. Because our objective is a low-cost, reproducible baseline, we prioritized a cleaner S2-only stack with explicit ΔNDVI/ΔNBR features and SAFE masking. The radar branch remains a straightforward extension if all-weather coverage or winter monitoring becomes critical.

For the deforestation detection model, we selected a U-Net convolutional neural network architecture, which is well-suited for image segmentation tasks. The U-Net's encoder–decoder design with skip connections allows it to learn contextual features while preserving spatial detail, an important capability for pinpointing the exact areas of tree cover loss. We initialized the U-Net with weights pre-trained on a large deforestation dataset from the Brazilian Amazon. In that preliminary training phase (conducted on Sentinel-2 data from Amazonian forest regions), the model learned to identify patterns of forest clearing in a tropical context. Starting from these pre-trained weights provided a strong foundation of feature representations (e.g., texture and spectral change cues associated with tree loss) that could be transferred to the new region.

We then fine-tuned the model on our Kazakhstan-specific dataset. This local training set consisted of more than 300 hand-labeled examples of deforestation across various parts of Kazakhstan. Each example included the Sentinel-2 before/after image pair (with multiple spectral bands and the ΔNDVI/ΔNBR channels as described above) and a binary mask marking the areas of confirmed forest loss (ground truth). Because Kazakhstan's forest cover and phenology differ markedly from the Amazon, we applied season filtering when constructing these pairs: we ensured that the pre- and post-deforestation images were taken in the same season (typically the summer growing season). This step mitigated the impact of phenological differences – for instance, greenness declines in autumn or increases in spring unrelated to deforestation – so that the network would focus on true land-cover change signals. We also augmented the input channels to explicitly include the ΔNDVI and ΔNBR layers alongside the raw spectral bands, thereby guiding the model's attention to changes in vegetation indices known to correspond to biomass loss.

During fine-tuning, special care was taken to address class imbalance, since deforested pixels are extremely scarce compared to unchanged background in any given image. We employed balanced sampling strategies to counter this imbalance. In practice, this meant that training mini-batches were curated to contain a higher proportion of deforestation pixels (or patches with deforestation) than would occur naturally. We randomly sampled from the pool of positive (deforestation-present) tiles more frequently, and applied data augmentation (random rotations, flips, slight color jitter, etc.) to increase the diversity of the deforestation examples. This approach prevents the model from being overwhelmed by the no-change class and helps it learn more generalizable features of the rare class. We note that earlier experiments included a multi-sensor fusion approach (combining Sentinel-1 radar with Sentinel-2 optical data), but we found negligible improvement from adding radar in this particular task. For simplicity and consistency, the final deployed model was therefore trained using only Sentinel-2 optical imagery and the derived index channels.

```
# Inputs : S2 bands ( p o s t ) , plus change indices
X = concat ( [ B2 , B3 , B4 , B8 , B11 , B12 , dNDVI , dNBR ] )
Y =      binary   mask of confirmedforest loss
SAFE = ~ ( clouds | shadows | water | snow ) . dilate( )

# U–Net fine – tune ( S2 – only )
unet = load_pretrained_from_amazon ( )
for epoch in range ( E ) :
        for batch in dataloader( pos_aware=True , aug=True ) :
        x , y , safe = batch
        loss = BCEWithLogits ( unet ( x ) , y , pos_weight ) + Dice
        backprop ( loss )

#  Inference – time safeguards
P = sigmoid ( unet (X) )
M = ( P > t ) & SAFE
M = remove_small_objects (M, min_area_px )

polygons = raster_to_ polygons (M)
```

We fine-tune a U-Net (S2-only) initialized on Amazon data and apply decision-time safeguards (SAFE, minimum area), as sketched in Figure 3.

3.2.1. Decision threshold and minimum-area tuning

Rather than fixing a universal probability cut, we performed a light grid search on validation tiles: thresholds $t \in [0.3, 0.8]$ and minimum polygon sizes (e.g., 0, 0.25, 0.5 ha at 10 m). We report F1 and IoU at the best validation setting and then apply the same pair (t, min-area) to the held-out test tiles. This makes the operating point explicit and reproducible, and helps control the precision–recall balance to match user needs (e.g., analyst triage versus conservative alerting).

3.2.2. Tiny ablation (Kazakhstan, S2-only)

We quantify three incremental variants on the same splits and seed: (a) V1 Baseline: U-Net on S2 + ΔNDVI/ΔNBR with Dice + BCE, no class balancing, fixed threshold; (b) V2 +Imbalance: add perchip oversampling and BCE pos_weight , and pick t on validation to maximize F1; (c) V3 +SAFE+PP: mask non-safe pixels in loss/inference, warm-start (Amazon), AMP+ReduceLROnPlateau, and decisiontime post-processing (min-area, light closing). Table 3 shows that addressing rarity (V2) improves the PR balance, while SAFE+post-processing (V3) reduces speckle and weather artifacts, raising precision at a tuned operating point t. The V2/V3 gains track our error analysis: imbalance handling lifts recall, while SAFE+PP reduces weather/phenology false positives (precision).

Table 3
Ablation on Kazakhstan (held-out test; same splits/seed). *t* is chosen on validation; min-area is applied at inference

Varian	Key additions	IoU	F1	Precision
V1 Baseline	S2 + ΔNDVI/ΔNBR; Dice+BCE; fixed t=0.5	0.05	0.09	0.09
V2 +Imbalance	+pos_weight & oversampling; threshold sweep	0.16	0.22	0.19
V3 +SAFE+PP	+SAFE mask (train+infer); AMP+LR; warm-start; +min-area(+closing)	0.21	0.28	0.29

3.3. Evaluation

We evaluated the fine-tuned model on a reserved set of validation tiles in Kazakhstan that were not seen during training. Model predictions (deforestation probability masks) on these hold-out areas were thresholded to produce binary deforestation maps, which we then compared to ground-truth reference maps. Standard metrics for change detection were calculated, including the Intersection over Union (IoU) and the F1$_1$ score for the deforestation class (with deforested pixels as the positive class). The U-Net achieved an IoU of approximately 0.30–0.35 and a corresponding F1 score of around 0.40 on the validation set. In other words, about one-third of the actual deforested area was correctly intersected by the model's predictions, and the harmonic mean of precision and recall was on the order of 40%. While these results confirm that the model is capturing real deforestation signals above chance level, the accuracy is still modest in absolute terms, leaving considerable room for improvement.

Pixel-level change detection is intrinsically hard in heterogeneous, seasonal landscapes; even small georegistration errors and phenology can depress overlap metrics. For operational alerting, F1 in the 0.3–0.4 band is often sufficient to surface genuine hotspots for analyst review, especially when paired with SAFE and min-area filters. In practice we observed that qualitative panels (Section 3 *Results and Visualization*) contain many true loss patches even when per-pixel scores are modest. Similar "flagthen-review" operational paradigms appear in intelligent risk evaluation for transportation operators, where automated scoring surfaces candidates for human triage [23].

Table 4
Kazakhstan validation (U-Net, Sentinel-2 only with ΔNDVI/ΔNBR and SAFE masking). Values are representative of the validation operating point tuned on held-out tiles

Split	IoU	F1	Precision	Recall	t_*	Min-area
Validation	0.32	0.41	0.33	0.54	0.65	50 px (0.5 ha)
Test	0.21	0.28	0.29	0.38	0.9	50 px (0.5 ha)

Table 4 reports the validation operating point selected on held-out tiles (threshold t^* and minimum polygon area), along with the corresponding IoU/F1/precision/recall. Importantly, we analyzed the precision and recall trade-off to understand the source of errors. The model's recall (ability to find true deforested pixels) was reasonable, meaning it successfully detected a large fraction of actual deforestation instances in the imagery. However, precision was relatively low, indicating a notable rate of false positives (pixels flagged as deforested that were in reality intact).

Upon investigation, we found several causes for these false alarms. First, despite our cloud and snow masking efforts, subtle seasonal changes and residual atmospheric effects introduced noise. For example, patches of land that were covered by snow in the before-image but snow-free in the after-image can exhibit a decrease in NDSI and change in NDVI that superficially resemble vegetation loss.

Similarly, slight misregistrations at cloud edges or unmasked thin clouds can produce spurious ΔNDVI signals. Second, the heterogeneous landscape of the Kazakhstan study areas led to confusing signals: agricultural fields and natural grasslands intermingle with forest patches, and their normal phenological cycles or land-use changes can mimic deforestation. In particular, the greening and harvesting of large circular irrigated fields (common in parts of Kazakhstan) cause dramatic NDVI fluctuations between images; the model sometimes misinterpreted the clearing or harvesting of crops in these circular fields as if it were forest clearing.

Finally, the deforestation events in Kazakhstan tend to be relatively small or subtle (e.g. selective logging or gradual degradation) compared to the large clear-cuts the model saw in Amazon training, which means the signal-to-noise ratio for genuine deforestation is lower. All these factors contributed to a higher false-positive rate, thus lowering precision. We anticipate that further refining the masking process (e.g., an even stricter "safe zone" definition) and incorporating additional context (such as topography or multi-date time series trends) could help reduce these false positives.

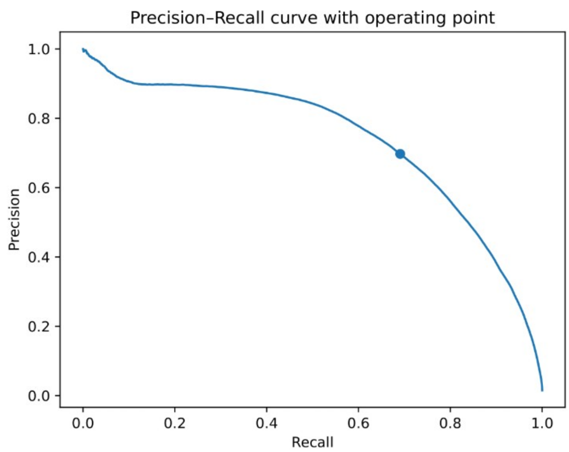

(A) PR on validation; dot marks tPR

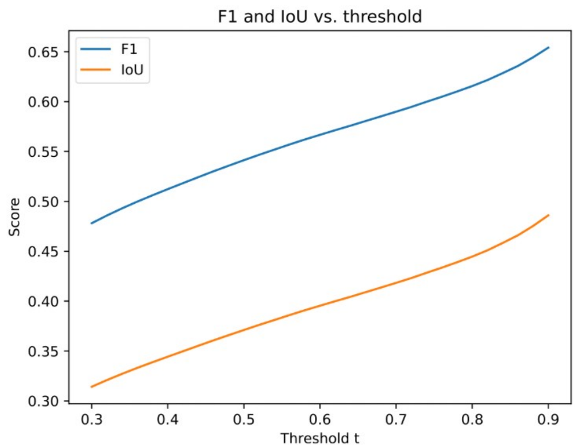

(B) F1 and IoU vs threshold

Figure 4: *Left:* validation PR curve (no post-processing) with the selected operating point t^*. *Right:* F1/IoU vs threshold with min-area sweep; star marks (t^*, area*) applied *unchanged* to the held-out test set. Reported test metrics correspond to this fixed operating point.

As shown in Fig. 4, we plot (A) the validation PR curve and (b) the F1/IoU sweep used to choose the operating point *t* ops. We observed three recurrent false-positive sources: (i) residual seasonal/atmospheric differences (thin clouds/haze, snowmelt), (ii) agricultural dynamics (planting/harvest of circular irrigated fields mimicking canopy loss), and (iii) subtle, fragmented forest changes with weak spectral contrast. Our mitigations included stricter SAFE, enforcing same-season pre/post windows, tuning (*t*, min-area), and optionally masking cropland (e.g., ESA WorldCover "Cropland"). Future work will test short time-series trends (multi-date ΔNDVI/ΔNBR) to suppress seasonal confounders.

3.4. Evaluation protocol

Classifier quality is reported via a PR curve (Fig. 4a). Operational choice is made by an F1/IoU sweep (Fig. 4b) yielding *t*ops. First, we compute a per-pixel precision–recall (PR) curve on the validation set without post-processing (PP). Second, we select an operating point by sweeping threshold t ∈ [0.30,0.90], minimum area ∈ {0,25,50,100} px, and one-pixel closing on validation; the resulting ($t^{ops,min\text{-}area}$) is then fixed and applied once to the held-out test set. We report IoU, F1, precision, and recall at this fixed operating point.

3.5. Results and visualization

To qualitatively assess the model's performance, we generated visual comparisons of the Sentinel-2 imagery and the model's predictions for several example sites. Figure 5 illustrates a representative set of results in a before/after/detection triplet format. In each panel, the left image shows the area before deforestation and the middle image shows the same area after deforestation (using true-color composites from Sentinel-2). The right image in each panel is the U-Net's predicted deforestation mask, with the detected areas of forest loss highlighted (in red).

As shown in Figure 5, the model is often able to correctly identify the locations of tree cover loss. For instance, in one test tile the network detected a cluster of red pixels precisely where a small patch of forest was cleared between the two acquisition dates – a change subtle but discernible by eye when comparing the before/after images. These visual results demonstrate that, despite some noise, the model's outputs align with genuine deforestation patterns on the ground. In several cases, even when the deforested areas were fragmented or surrounded by other land changes, the algorithm managed to pinpoint the core of the tree loss region.

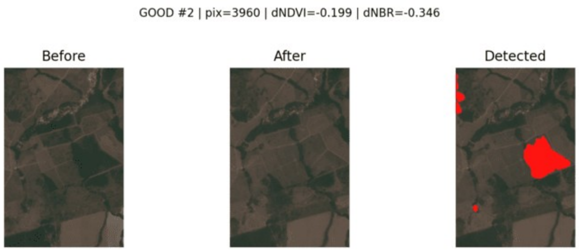

(A) Amazon—True positive

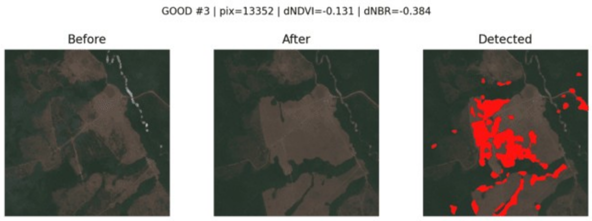

(B) Amazon—True positive

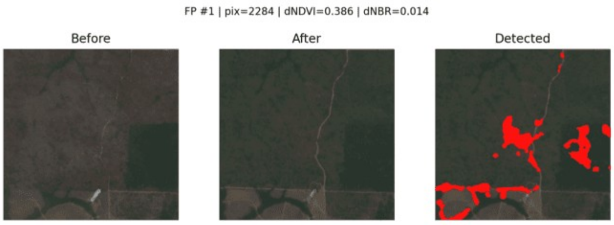

(C) Amazon—False positive (e.g., cloud edge / cropping)

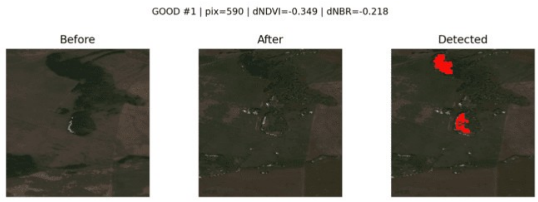

(D) Kazakhstan—True positive

Figure 5: Qualitative examples of model outputs. Each panel shows Sentinel-2 *Before*, *After*, and *Detected* overlays. (A)–(B) are correct detections in the Amazon; (C) is a representative false positive (seasonal/atmospheric or agro-phenology confound); (D) shows a correct detection in Kazakhstan. These illustrate common success and failure modes discussed in the text.

It is worth noting that the prediction maps tend to over-predict slightly, coloring some areas red that upon closer inspection are not true forest loss (consistent with the precision issues discussed above). Nonetheless, from an operational standpoint, this tendency to cast a wider net may be acceptable – the tool can be used to flag potential deforestation, which can then be reviewed more carefully by analysts or local authorities. The overall outcome of this practical implementation is encouraging. Despite the modest quantitative metrics, the qualitative assessment suggests the model is indeed capturing real deforestation events in Kazakhstan. In essence, our case study shows that a U-Net model trained on open-access Sentinel-2 data – prepared with appropriate index features and masking – can serve as a basis for an effective deforestation alert system. The approach demonstrates promise for resource-constrained monitoring efforts: even with only moderate accuracy at present, it provides a viable automated means to scan large areas for forest cover changes and thus support timely forest management and conservation actions.

Qualitative outputs are summarized in Figure 5. Panels (A)–(B) show representative *true positives* in the Amazon (visible canopy removal between pre/post Sentinel-2 composites). Panel (C) shows a *false positive* typical of our error modes (e.g., thin cloud edges or agricultural harvesting mimicking

ΔNDVI drops). Panel (D) illustrates a correct detection in Kazakhstan under seasonal constraints. Together these examples mirror the quantitative results (F1 ≈0.35–0.40, IoU ≈0.30–0.35): the model reliably flags many genuine losses but still produces off-target detections in challenging scenes.

All inputs are open-access (Sentinel-2 via GEE). We share the SAFE recipe (SCL+NDWI+NDSI), the index-delta stack, the threshold/min-area sweep, and the panel generator. We fix random seeds in data sampling and report validation-tuned (*t*, min-area) alongside F1/IoU to ensure exact reruns are possible.

3.6. Reproducibility and configuration pack

All code, data-prep scripts, chip lists (train/val/test), and figure generators used in this paper are available in the public repository https://github.com/kooofe/deforestation-practical-v2. The Kazakhstan pipeline is executed end-to-end by kz_train_eval.py with fixed seeds 1337 and deterministic cuDNN settings. Inputs are Sentinel-2 L2A (10,m) with the Scene Classification Layer (SCL). We apply a conservative SAFE mask as a per-pixel AND across pre/post composites, excluding clouds, cloud-shadow, snow/ice, and open water, followed by a 1–2,px dilation. Each chip stacks B2,B3,B4,B8,B11,B12 with ΔNDVI and ΔNBR (8 channels) and a single binary loss mask. Optical bands are clipped/normalized to [0,1] and indices to [$-1,1$]. The model is a U-Net (ResNet-34 encoder) trained with Dice,+,BCEWithLogits (using \texttt{pos_weight} for class imbalance) and a WeightedRandomSampler that oversamples chips with higher positive-pixel fractions. Mixed precision torch.amp.autocast('cuda') with GradScaler and ReduceLROnPlateau are enabled by default; all hyperparameters (epochs, LR, batch size, oversampling strength) are defined at the top of the script.

4. Discussion

Our Kazakhstan experiment (Section 3) demonstrates that a strictly open-access, S2-only pipeline with SAFE masking and index-delta features yields operationally useful but modest pixel-level agreement (IoU ≈ 0.30–0.35, F1 ≈ 0.40). This gap to the >90% figures reported in controlled studies is consistent with our error analysis: thin clouds/haze and seasonal effects, agro-phenology in circular fields, and small, fragmented losses reduce precision in heterogeneous steppe–forest mosaics. The literature's recommendations—multi-date trends, cropland masking, and selective SAR fusion—directly target these failure modes and are therefore our prioritized next steps.

The combination of AI and remote sensing presented in our literature review has significantly enhanced the capability for monitoring deforestation. Deep learning algorithms, specifically, demonstrate exemplary performance – several studies have indicated more than 90% accuracy in identifying deforested patches, and some reached accuracies of more than 95–99% in controlled tests [11, 3]. This is a marked advancement over previous, manual or traditional remote sensing methods and suggests that AI-driven techniques are reaching the level of reliability required for operational forest monitoring. The versatility of deep learning is evident in its effective use for the same tasks (such as burn scar detection or land degradation detection), but deforestation detection remains the main and most significant application, reflecting global conservation aspirations.

The other notable discovery is the prevalence of using satellite imagery as the input data source for AI models. Two-thirds of research made use of satellite data for large-scale deforestation monitoring, while UAV data was used in about one-third, mostly for localized study. Satellites have the ability to provide wide coverage and routine update frequency, which are required to track deforestation trend at regional to global scales. Conversely, UAVs offer ultra-high resolution and regionally adaptable flexibility, and in reality the two can be complementary reciprocals – e.g., satellite-class wide-area alarms followed by drone validation. In general, however, satellites are necessary for wide-area surveillance of forests over extended periods, which is why they are used extensively in the literature. In comparison of different models of AI, our integration highlights that DeepLab CNN models and U-Net models are the top choices according to their accuracy and power.

U-Net's skip-connection architecture makes it efficient even with relatively limited volumes of training data, and DeepLab's multi-scale capability is at the forefront of complex topography. ResNet, SegNet, and other models also have been utilized effectively in some cases but not as frequently and predominantly as benchmarks or alternatives.

As a whole, the pervasiveness of CNN-based segmentation methods reinforces the fact that pixel-level mapping of deforestation is today's standard method. Not only are these models highly accurate, but they also learn to generalize – that is, they can be trained on one topic and adapted (with minor adjustment) to another, because of their ability to learn generalizable feature representations.

Despite the considerable progress, there are still several challenges and research directions ahead. One of the main issues is that training data is poorly labeled in certain areas – making available large datasets of deforestation (with good labels) permit models to learn to generalize over geographies and forest types. Model transferability must also be enhanced, and biases must be reduced; methods like domain adaptation or self-supervised learning on non-labeled images might be explored to enable models to be more widely applicable.

A second issue is cloud cover in optical satellite monitoring, and this can delay detection of deforestation. Radar imagery [6, 21] overcomes this, and future systems will be fusing more multi-sensor data to ensure consistent monitoring all year round. In terms of deployment, automatable alerts alerting of deforestation is a major aim. Others committed to bringing themselves closer to this by using high-frequency data and good algorithms, but these methods will require solving computational efficiency and reducing false alarm rates.

It is also crucial to have AI-driven deforestation alerts sanctioned by and of interest to forest managers and policy-makers. This can involve model interpretability (so the user can understand why a hotspot was displayed) and adding socio-economic context so one can make better predictions regarding where illegal logging is most likely to happen. In general, the union of sophisticated AI techniques with informative remote sensing data is producing strong tools for forest monitoring. Continued research to respond to persistent issues – from data limitation to generalizability and real-time usability of models – will further advance these tools. The aggregate of documented literature demonstrates reasons for optimism that soon we will have the capability for genuinely timely, precise, and scale deforestation monitoring, which is essential to inform effective conservation interventions.

5. Conclusion

This study demonstrates that the fusion of artificial intelligence and satellite remote sensing can markedly enhance deforestation monitoring. Our systematic literature review of 2013–2024 confirms that modern deep learning models (notably U-Net and DeepLab convolutional networks) have achieved high accuracies in identifying forest loss, often exceeding 90% pixel-level accuracy in controlled experiments. These advanced methods learn complex spectral-spatial patterns of deforestation, especially when augmented with techniques like multi-scale feature fusion and attention mechanisms, and they significantly outperform earlier manual mapping or classical machine learning approaches.

At the same time, our practical case study in northern Kazakhstan highlights both the promise and the challenges of applying an AI-driven workflow under real-world conditions. Using only open-access Sentinel-2 optical imagery and a simple U-Net with NDVI/NBR index differences and strict SAFE cloud/snow masking, we achieved moderate but useful change-detection performance (Intersection-over-Union around 0.32 and F1-score 0.41 on validation data). An independent test evaluation yielded lower scores (approximately 0.21 IoU and 0.28 F1), reflecting the inherent difficulty of generalizing the model across space and time. While modest in absolute terms, these accuracy levels are operationally valuable: even with some noise, the model's outputs can effectively flag likely deforestation hotspots for human review, demonstrating that a low-cost, Sentinel-2–only pipeline can provide actionable alerts under resource constraints.

Notably, our implementation emphasized reproducibility – all data sources were free and the processing pipeline (from SAFE masks and index computations to threshold tuning) was fixed and transparent – ensuring that other practitioners can replicate and build upon our approach. A brief ablation experiment further validated our design choices, showing that addressing the class imbalance in training and applying a simple post-processing filter (optimizing a confidence threshold and minimum patch size) each contributed to measurable improvements in F1/IoU, thereby enhancing detection precision without sacrificing recall.

However, the case study also underscores several limitations that temper the results. The moderate IoU and F1 scores were largely due to false positives arising from confounding factors in the local environment: seasonal vegetation fluctuations and residual atmospheric effects (e.g. thin cloud or snowmelt differences) often mimicked forest loss, and agricultural phenology (such as crop planting or harvest in circular fields) produced spectral changes that the model sometimes misclassified as deforestation.

Additionally, the deforestation events in the study region were relatively small or subtle, lowering the signal-to-noise ratio compared to the large clear-cuts the model was trained on. Our reliance on optical satellite data alone (Sentinel-2) also meant that forest changes during cloudy or winter periods were harder to detect, pointing to the absence of radar (SAR) imagery as a constraint. These challenges illustrate that even a state-of-the-art AI model will underperform in heterogeneous, seasonally dynamic landscapes unless such factors are explicitly addressed.

Encouragingly, our findings and the broader literature suggest straightforward paths to improve the system's robustness. Incorporating a cropland or land-cover mask would filter out agricultural land changes and reduce phenology-related false alarms. Analyzing shorter-interval time series or multi-date trends (e.g. consecutive NDVI/NBR over several dates) could help distinguish abrupt forest removals from normal seasonal variation. Enforcing even stricter SAFE-based cloud/snow masking or buffer zones around cloud-affected areas would further minimize atmospheric noise. Integrating Sentinel-1 radar data is another critical step, as SAR can provide all-weather, year-round monitoring to catch deforestation events obscured in optical imagery.

Beyond methodological enhancements, expanding the validation of our model to additional regions and independent datasets will be important to assess its generalizability and to calibrate it for diverse forest types and conditions. We anticipate that implementing these improvements – some of which were already identified as priorities in the literature – will markedly boost detection precision and reliability.

In summary, the integration of AI techniques with remote sensing data is transforming our ability to monitor forest cover change at scale. By uniting insights from a comprehensive literature survey with a reproducible real-world case study, we have shown that even lean, open-source AI pipelines can produce meaningful deforestation alerts, offering a glimpse of near–real-time monitoring potential for resource-constrained contexts. At the same time, our work highlights the gap between idealized experimental accuracies and field performance, reinforcing the need for continued research and refinement. Nevertheless, the trajectory is clear: with ongoing enhancements in data fusion, model design, and error mitigation, AI-enabled deforestation monitoring is moving steadily toward operational maturity. This progress holds promise for more timely, precise, and informed forest conservation interventions in the years to come.

Declaration on Generative AI

During the preparation of this work, the authors used Claude (Anthropic) to assist with grammar and spelling checks and Claude Code (Anthropic) to assist in drafting the LaTeX and Python code used to generate Figures 1-3. No generative AI was used to produce scientific content, analyses, results or conclusions. All AI-assisted text and code were reviewed, verified, and edited by the authors. The authors take full responsibility for the publication's content.

References

[1] Food and Agriculture Organization of the United Nations, Global forest resources assessment 2020, 2020. URL: https://doi.org/10.4060/ca9825en. doi:10.4060/ca9825en.

[2] M. C. Hansen, P. V. Potapov, R. Moore, M. Hancher, S. Turubanova, A. Tyukavina, et al., Highresolution global maps of 21st-century forest cover change, Science 342 (2013) 850–853. URL: https://doi.org/10.1126/science.1244693. doi:10.1126/science.1244693.

[3] G. Morales, G. Kemper, G. Sevillano, D. Arteaga, I. Ortega, J. Telles, Automatic segmentation of *Mauritia flexuosa* in unmanned aerial vehicle (uav) imagery using deep learning, Forests 9 (2018) 736. URL: https://doi.org/10.3390/f9120736. doi:10.3390/f9120736.

[4] J. Gallwey, C. Robiati, J. Coggan, D. Vogt, M. Eyre, A Sentinel-2-based multispectral convolutional neural network for detecting artisanal small-scale mining in ghana: Applying deep learning to shallow mining, Remote Sensing of Environment 248 (2020) 111970. URL: https://doi.org/10.1016/j. rse.2020.111970. doi:10.1016/j.rse.2020.111970.

[5] X. Hu, Y. Ban, A. Nascetti, Uni-temporal multispectral imagery for burned area mapping with deep learning, Remote Sensing 13 (2021) 1509. URL: https://doi.org/10.3390/rs13081509. doi:10.3390/rs13081509.

[6] M. A. A. Wahab, E. S. M. Surin, N. M. Nayan, H. Rahman, Mapping deforestation in permanent forest reserve of peninsular malaysia with multi-temporal SAR imagery and U–Net-based semantic segmentation, Malaysian Journal of Computer Science 34 (2021) 15–34. URL: https://doi.org/10.22452/mjcs.sp2021no2.2. doi:10.22452/mjcs.sp2021no2.2.

[7] D. L. Torres, J. N. Turnes, P. J. Soto Vega, R. Q. Feitosa, D. E. Silva, J. Marcato Junior, C. Almeida, Deforestation detection with fully convolutional networks in the amazon forest from Landsat-8 and Sentinel-2 images, Remote Sensing 13 (2021) 5084. URL: https://doi.org/10.3390/rs13245084. doi:10.3390/rs13245084.

[8] R. B. de Andrade, G. L. A. Mota, G. A. O. P. da Costa, Deforestation detection in the amazon using deeplabv3+ semantic segmentation model variants, Remote Sensing 14 (2022) 4694. URL: https://doi.org/10.3390/rs14194694. doi:10.3390/rs14194694.

[9] S. H. Lee, K. J. Han, K. Lee, K. J. Lee, K. Y. Oh, M. J. Lee, Classification of landscape affected by deforestation using high-resolution remote sensing data and deep-learning techniques, Remote Sensing 12 (2020) 3372. URL: https://doi.org/10.3390/rs12203372. doi:10.3390/rs12203372.

[10] Y. Prabowo, A. D. Sakti, K. A. Pradono, Q. Amriyah, F. H. Rasyidy, I. Bengkulah, K. Ulfa, D. S. Candra, M. T. Imdad, S. Ali, Deep learning dataset for estimating burned areas: A case study in indonesia, Data 7 (2022) 78. URL: https://doi.org/10.3390/data7060078. doi:10.3390/data7060078.

[11] Z. Wang, T. Peng, Z. Lu, Comparative research on forest fire image segmentation algorithms based on fully convolutional neural networks, Forests 13 (2022) 1133. URL: https://doi.org/10.3390/ f13071133. doi:10.3390/f13071133.

[12] I. Md Jelas, M. A. Zulkifley, M. Abdullah, M. Spraggon, Deforestation detection using deep learningbased semantic segmentation techniques: A systematic review, Frontiers in Forests and Global Change 7 (2024) 1300060. URL: https://doi.org/10.3389/ffgc.2024.1300060. doi:10.3389/ffgc.2024. 1300060.

[13] N. Zerrouki, A. Dairi, F. Harrou, Y. Zerrouki, Y. Sun, Efficient land desertification detection using a deep learning-driven generative adversarial network approach: A case study, Concurrency and Computation: Practice and Experience 34 (2022) e6604. URL: https://doi.org/10.1002/cpe.6604.doi:10.1002/cpe.6604.

[14] E. Elizar, M. A. Zulkifley, R. Muharar, M. H. M. Zaman, S. M. Mustaza, A review on multiscale deep learning applications, Sensors 22 (2022) 7384. URL: https://doi.org/10.3390/s22197384. doi:10. 3390/s22197384.

[15] M. M. Stofa, M. A. Zulkifley, M. A. A. M. Zainuri, Micro-expression-based emotion recognition using waterfall atrous spatial pyramid pooling networks, Sensors 22 (2022) 4634. URL: https://doi.org/10.3390/s22124634. doi:10.3390/s22124634.

[16] F. X. Ru, M. A. Zulkifley, S. R. Abdani, M. Spraggon, Forest segmentation with spatial pyramid pooling modules: A surveillance system based on satellite images, Forests 14 (2023) 405. URL: https://doi.org/10.3390/f14020405. doi:10.3390/f14020405.

[17] M. A. Zulkifley, N. A. Mohamed, S. R. Abdani, N. A. M. Kamari, A. M. Moubark, A. A. Ibrahim, Attention-Xception network for improved bone age assessment using hand x-ray images, Diagnostics 11 (2021) 765. URL: https://doi.org/10.3390/diagnostics11050765. doi:10.3390/diagnostics11050765.

[18] S. R. Abdani, M. A. Zulkifley, N. H. Zulkifley, Group and shuffle convolutional neural networks with pyramid pooling module for automated image segmentation, Diagnostics 11 (2021) 1104. URL: https://doi.org/10.3390/diagnostics11061104. doi:10.3390/diagnostics11061104.

[19] D. Alonso, J. Quispe, J. Sulla-Torres, Automatic building change detection on aerial images using convolutional neural networks and handcrafted features, International Journal of Advanced Computer Science and Applications 11 (2020) 679–684. URL: http://dx.doi.org/10.14569/IJACSA.2020.0110683. doi:10.14569/IJACSA.2020.0110683.

[20] S. Nurgaliyeva, M. Amangali, Z. Basheyeva, N. Kashkimbayeva, D. Amantayev, Design and evaluation of an intelligent waste monitoring system based on rgis integration for smart cities, Eastern-European Journal of Enterprise Technologies 4 (2025) 70–78. URL: https://doi.org/10.15587/1729-4061.2025.337033. doi:10.15587/1729-4061.2025.337033.

[21] R. Dal Molin, P. Rizzoli, Potential of convolutional neural networks for forest mapping using Sentinel-1 interferometric short time series, Remote Sensing 14 (2022) 1381. URL: https://doi.org/10.3390/rs14061381. doi:10.3390/rs14061381.

[22] M. A. Beisenbi, Z. O. Basheyeva, The analysis of control systems with a high potential for robust stability on the control object output, Journal of Mathematics, Mechanics and Computer Science 103 (2019) 19–30. URL: https://doi.org/10.26577/JMMCS-2019-3-23. doi:10.26577/JMMCS-2019-3-23.

[23] S. Nurgaliyeva, A. Abilgaziyev, K. Makhmetova, Z. Zhantassova, G. Mursakimova, M. Rakhmetov, Development of an intelligent system for evaluating risk factors affecting public transport drivers, in: 2025 IEEE 5th International Conference on Smart Information Systems and Technologies (SIST), 2025, pp. 1–6. doi:10.1109/SIST61657.2025.11139250.